

Design of Crane Runway Beam with Channel Cap

DUANE S. ELLIFRITT and DUNG-MYAU LUE

INTRODUCTION

A common practice in industrial buildings is to weld a channel, open side down, to the top flange of a standard rolled beam for use as a crane runway. In many cases, it is not possible to brace a crane runway laterally between columns, so the channel provides additional lateral stiffness.

There are several interesting structural questions associated with the practice, like, what should be the welding pattern? How are the residual stresses affected? What if the channel has a yield strength different from the beam? However, the primary question addressed in this paper is, how does one check such a beam for lateral-torsional buckling?

The AISC Specification provides formulas for lateral-torsional buckling of monosymmetric sections, but these are derived for three-plate sections, as shown in Figure 1(a). Some of these equations require the calculation of section properties that are not readily available from handbooks, like the warping constant, nor do they apply to the real section as shown in Figure 1(b).

The purpose of this research was to develop an analytical solution to the problem of lateral-torsional buckling of a rolled beam with channel cap in terms that are readily available from standard section property tables. A program of full-scale testing was carried out to verify the analytical solution. It should be noted here that the solution proposed in this paper applies only to light- to medium-duty cranes, those classified as A, B, or C by the Crane Manufacturers Association of America (CMAA).

ANALYTICAL SOLUTION FOR ELASTIC BUCKLING

According to Clark and Hill (1960), Galambos (1968 & 1988), and Johnston (1976), the elastic nominal moment (M_n) of a monosymmetric beam, including the section of a rolled beam with a channel cap, can be expressed by the following equations:

$$M_n = \frac{\pi C_b}{KL} \left\{ \sqrt{EI_y GJ} \left(B_1 + \sqrt{1 + B_2 + B_1^2} \right) \right\} \quad (1)$$

where

$$B_1 = \frac{\pi \beta_x}{2KL} \sqrt{\frac{EI_y}{GJ}} \quad (2)$$

$$B_2 = \frac{\pi^2 EC_w}{(KL)^2 GJ} \quad (3)$$

$$\beta_x = \frac{1}{I_x} \int_A y(x^2 + y^2) dA - 2y_o \quad (4)$$

$$C_w = \int_o^L W_n^2 t ds, W_n = \frac{1}{A} \int_o^L W_o t ds - W_o, W_o = \int_o^s \rho_o ds \quad (5)$$

$$J = \int_A r^2 dA \quad (6)$$

K = effective length factors (Assume $K_x = K_y = K_z = 1.0$)

To evaluate the elastic nominal moment (M_n) according to Equations 1, 2, and 3, one has to determine the coefficient of

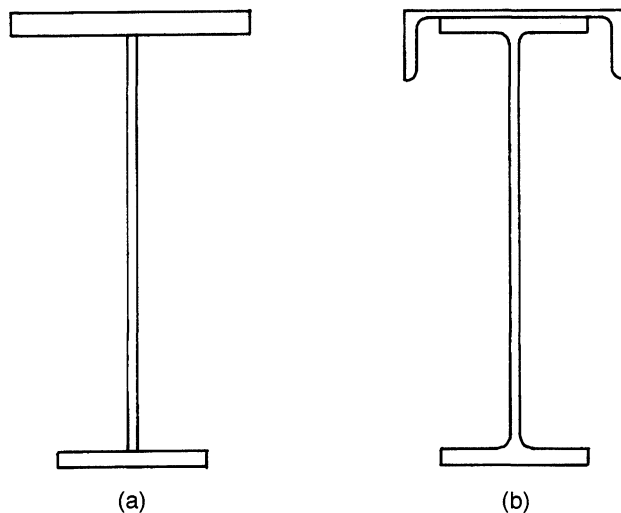


Fig. 1. Common monosymmetric sections: (a) 3-plate section, (b) rolled beam with channel cap.

Duane S. Ellifritt is professor of structural design, University of Florida, Gainesville, FL.

Dung-Myau Lue is associate professor, National Chung-Hsing University, Taiwan.

monosymmetry (β_x), the warping constant (C_w), and the torsional constant (J).

For a monosymmetric section made of three dissimilar plates, Equations 2 and 3 can be simplified into

$$B_1 = 2.25 \left[2 \left(\frac{I_{yc}}{I_y} \right) - 1 \right] \left(\frac{h}{L_b} \right) \sqrt{\frac{I_y}{J}} \quad (7)$$

$$B_2 = 25 \left(1 - \frac{I_{yc}}{I_y} \right) \left(\frac{I_{yc}}{J} \right) \left(\frac{h}{L_b} \right)^2 \quad (8)$$

In this way, the need to calculate the warping constant is avoided. Equations 7 and 8 are identical to the equations in the footnote on page 6-114 of the AISC-LRFD Specification (1993).

However, these equations are correct only for the three-plate section; they are conservative for the section which is the subject of this paper. For the beam-and-channel section, one should calculate β_x , C_{wc} , and J according to Equations 4, 5 and 6, but this can be a daunting task for routine design office use. It would be better to have models for these three items which make use of known properties, or easy-to-find properties, that are still reasonably accurate.

PROPOSED MODELS

The β_x Model

According to Kitipornchai and Trahair (1980), β_x for a section with a lipped top flange is given by

$$\beta_x = 0.9h \left(\frac{2I_{yc}}{I_y} - 1 \right) \left(1 - \left(\frac{I_y}{I_x} \right)^2 \right) \left(1 + \frac{D_L}{2D} \right) \quad (9)$$

Recognizing that $(I_y/I_x)^2$ is a very small number, and letting $h = D$, this equation can be reduced to

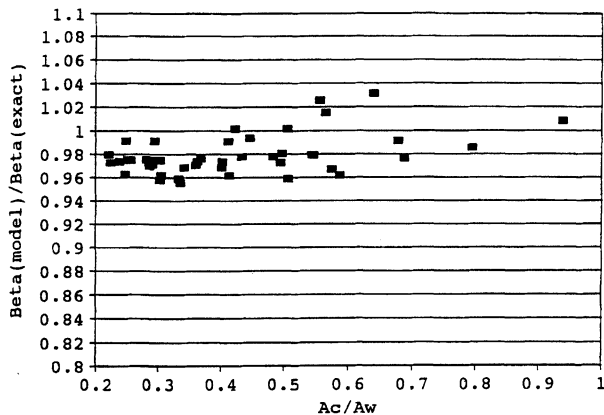


Fig. 2. The accuracy of the β_x model.

$$\beta_x = 0.9 \left(\frac{2I_{yc}}{I_y} - 1 \right) \left(D + \frac{D_L}{2} \right) \quad (10)$$

Using the forty-five sections shown in the AISC Manual (AISC, 1989) as a data base, it was found that Equation 11 gave a very close approximation of Equation 9

$$\beta_x = 0.87(R - 1) \left(D + \frac{D_L}{2} \right) \quad (11)$$

where

$$R = \frac{2I_{yc}}{I_y}$$

The solution (Kitipornchai and Trahair) and the proposed model are plotted in Figure 2. It can be seen that the approximate model (Equation 11) is accurate within ± 4 percent.

The C_{wc} Model

The authors used a computer program originally written in BASIC language by Dr. T. V. Galambos, to calculate the exact values of warping constants (C_{wc}) of a beam with a channel cap. The results for the forty-five sections shown in the AISC manuals (AISC 1989 and AISC 1993) are plotted in Figure 3. By applying a multiple linear regression technique to the data, the following curve was found to be a good fit.

$$C_{wc} = C_w \left(0.79 + 1.79 \sqrt{\frac{A_c}{A_w}} \right) \quad (12)$$

where

$$0.2 \leq \frac{A_c}{A_w} \leq 0.95$$

The resulting curve is superimposed on the data of Figure 3. The model as given by Equation 12 requires no calculation of

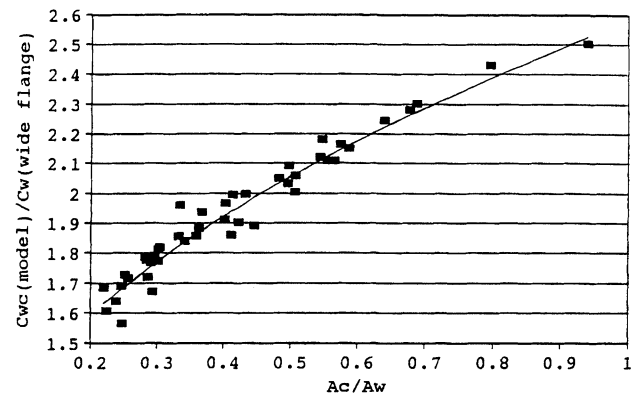


Fig. 3. The warping constant model as a function of beam and channel area.

section properties and uses only C_w and the ratio A_c/A_w as the independent variables. These variables A_c , A_w , and C_w are given in the AISC *Manual of Steel Construction*. In Figure 4, it can be observed that the model gives results with errors of -3 percent to +5 percent in most sections. [It should be noted that Equation 12 is slightly different from the formula published by Lue and Ellifritt (Lue, 1993) previously. This equation is more accurate, while retaining the simplicity of the one published in 1993.]

The J Model

The torsional constant (J) can be expressed by

$$J = \int_A r^2 dA = \frac{1}{3} \sum_1^n b_i t_i^3 \quad (13)$$

where

- b_i and t_i = width and thickness, respectively of each element of the cross-section
- n = number of plate elements

A further modification of Equation 13 has been done for the need of the practical designer. The modified formula of J is calculated based on the section properties and dimensions of wide flanges and channel caps as listed in AISC manual. The proposed J is given by the following equations.

$$J = \frac{1}{3} \sum_0^n b_i t_i^3 = J_w + J_c + \frac{1}{3} b_f (t_1 + t_2)^3 - \frac{1}{3} b_f (t_1^3 + t_2^3) \quad (14)$$

$$= J_w + J_c + b_f t_1 t_2 (t_1 + t_2) \quad (15)$$

where

- J_w and J_c = torsional constants for the wide flange and the channel, respectively
- b_f = flange width of the wide flange
- t_1 = web thickness of the channel

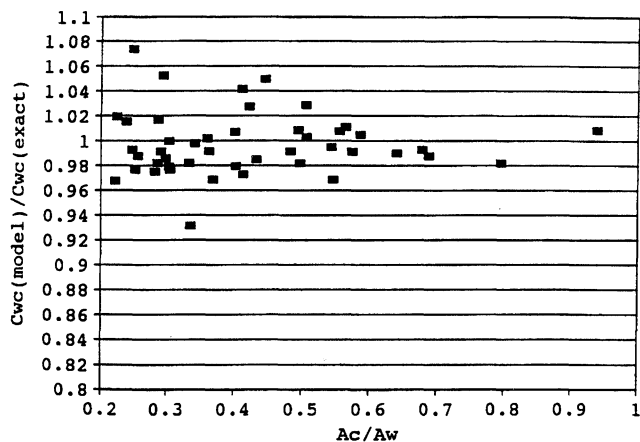


Fig. 4. The accuracy of the warping constant model.

t_2 = flange thickness of the wide flange

All the variables shown are listed in the AISC manual.

Again, the model is applied to the forty-five sections in the AISC Manual and the results are plotted in Figure 5. It can be seen that the model overestimates the value of J by +2.1 percent to +8.2 percent.

APPROXIMATE DESIGN USING THE PROPOSED MODELS

The proposed models based on the previous discussions can be summarized by the following equations.

$$M_n = \frac{\pi C_b}{KL} \left[\sqrt{EI_y GJ} \left(B_1 + \sqrt{1 + B_2 + B_1^2} \right) \right] \quad (16)$$

where

$$B_1 = \frac{\pi \beta_x}{2KL} \sqrt{\frac{EI_y}{GJ}} \quad B_2 = \frac{\pi^2 EC_{wc}}{(KL)^2 GJ} \quad (17)$$

$$\beta_x = 0.87(2R - 1) \left(D + \frac{D_L}{2} \right), \quad R = \frac{2I_{yc}}{I_y} \quad (18)$$

$$I_y = I_{yw} + I_{xc}, \quad I_{yc} = \frac{I_{yw}}{2} + I_{xc} \quad (19)$$

$$C_{wc} = C_w \left(0.79 + 1.79 \sqrt{\frac{A_c}{A_w}} \right), \quad 0.2 \leq \frac{A_c}{A_w} \leq 0.95 \quad (20)$$

$$J = J_w + J_c + B t_1 t_2 (t_1 + t_2) \quad (21)$$

The forty-five AISC sections are used to examine the differences between the exact nominal moments (M_n) and the ones based on the proposed models.

The curves of nominal moment (M_n) versus unbraced length (L_b) were examined by using the proposed models. A

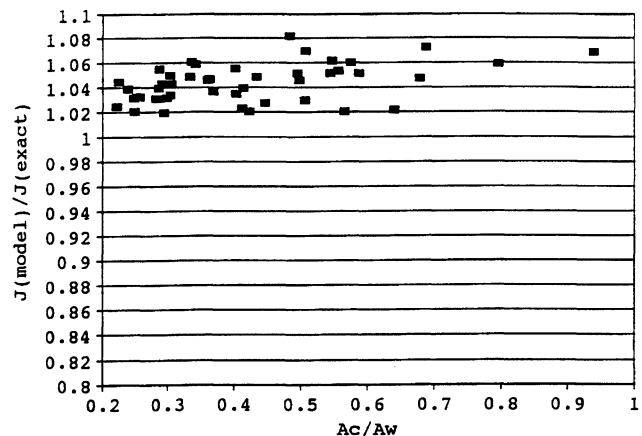


Fig. 5. The accuracy of the torsion constant model.

straight line, which is adopted by the current LRFD method, is used for the inelastic nominal moment between the plastic moment (M_p) and the limiting moment (M_r). The results of the twenty-eight sections in the AISC-LRFD Manual are recorded in Table 1. It can be seen that the model gives errors of -2.5 percent to $+1.8$ percent.

The proposed formulation, shown in Equations 16 through 21, makes use of only dimensions and properties readily available from the AISC Manual and produces results only ± 2.5 percent from the exact solution.

Bear in mind that the foregoing is only an *elastic* solution and the increased lateral strength of adding a channel cap may mean that lateral-torsional buckling will be *inelastic*. However, the inelastic transition curve will still be affected by the elastic curve. In this research, the AISC-LRFD approach of using a straight line inelastic transition curve between M_p and M_r was followed.

Experimental Study

Full-scale tests were performed on the beams shown in Table 3. The testing apparatus is shown in Figure 6. The beams were tested with a single concentrated load applied to the top flange through a ball joint either at mid-span or at the one third-point. A gravity load simulator, as shown in Figure 6, was used to ensure that the load would remain vertical during lateral buckling of the beam. An independent stand held two LVDT's for measuring both vertical and horizontal displacements. The ends of the beams rested on rollers and could rotate about both horizontal and vertical axes, but were restrained from torsional rotation about a longitudinal axis.

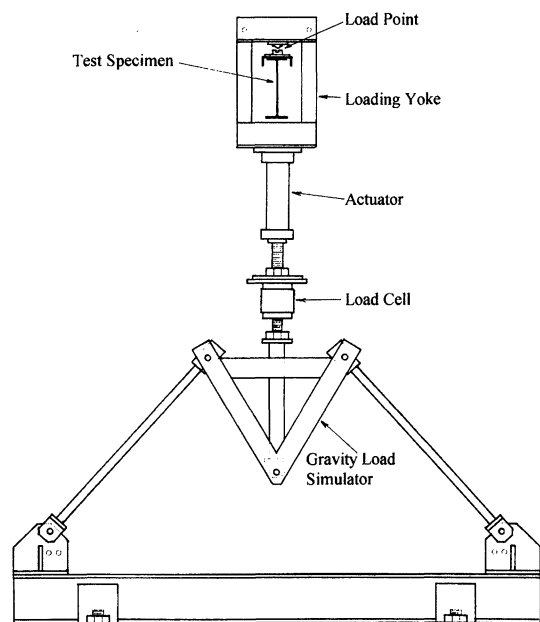


Fig. 6. Experimental loading apparatus.

Table 1.
Percent Error in Proposed Elastic Buckling Moment Model for Combination Beam and Channel Sections Shown in the AISC-LRFD Manual (1993)

Beam	Channel	A_c / A_w	% Error
920×223 (36×150)	380×50 (15×33.9)	0.225	-0.8 to -0.1
840×210 (33×141)	380×50 (15×33.9)	0.239	-0.9 to -0.2
610×125 (24×84)	310×31 (12×20.7)	0.247	-1.8 to -0.7
920×223 (36×150)	460×64 (18×42.7)	0.285	-1.4 to -0.4
840×176 (33×118)	380×50 (15×33.9)	0.287	-1.1 to -0.3
760×173 (30×116)	380×50 (15×33.9)	0.291	-1.3 to -0.4
840×210 (33×131)	460×64 (18×42.7)	0.303	-1.3 to -0.7
610×101 (24×68)	310×31 (12×20.7)	0.303	-2.1 to -1.0
530×101 (21×68)	310×31 (12×20.7)	0.305	-1.9 to -0.5
530×92 (21×62)	310×31 (12×20.7)	0.333	-2.0 to -0.5
760×147 (30×99)	380×50 (15×33.9)	0.342	-1.4 to -0.4
690×140 (27×94)	380×50 (15×33.9)	0.360	-1.2 to -0.5
840×176 (33×118)	460×64 (18×42.7)	0.363	-1.3 to -0.5
760×173 (30×116)	460×64 (18×42.7)	0.368	-1.2 to -0.5
690×125 (27×84)	380×50 (15×33.9)	0.402	-1.2 to -0.3
610×125 (24×84)	380×50 (15×33.9)	0.403	-1.2 to -0.5
460×74 (18×50)	310×31 (12×20.7)	0.414	-2.0 to -0.8
760×147 (30×99)	460×64 (18×42.7)	0.433	-1.0 to -0.2
610×101 (24×68)	380×50 (15×33.9)	0.496	-1.1 to -0.2
530×101 (21×68)	380×50 (15×33.9)	0.498	-0.6 to +0.1
360×44 (14×30)	250×23 (10×15.3)	0.507	-1.2 to +0.2
530×92 (21×62)	380×50 (15×33.9)	0.544	-0.5 to +0.1
410×53 (16×36)	310×31 (12×20.7)	0.575	-0.4 to +1.4
310×39 (12×26)	250×23 (10×15.3)	0.587	-2.5 to -0.8
460×74 (18×50)	380×50 (15×33.9)	0.678	+0.1 to +0.6
360×44 (14×30)	310×31 (12×20.7)	0.688	-0.4 to +0.6
310×39 (12×26)	310×31 (12×20.7)	0.796	-1.6 to -1.3
410×53 (16×36)	380×50 (15×33.9)	0.940	+0.4 to +1.8

Notes: A_c = Area of Channel A_w = Area of Beam
 F_y = 350 MPa (50 ksi)
Unbraced Length = 19 to 23 m (60 to 70 ft.)
 M_{n1} = Theoretical Nominal Moment
 M_{n2} = Nominal Moment by Proposed Model
% Error = $(M_{n2} - M_{n1}) / M_{n1} * 100$

In selecting the beam and channel sizes to be tested, an attempt was made to devise combined specimens that represented low, intermediate and high values of the area ratios (See Table 1 for representative values of A_c / A_w).

In order to get the most out of the material, each beam was tested twice: once without the channel cap, and once with it. In the first test, the beam was made long enough to ensure buckling in the elastic range. Then it was unloaded, taken down and a channel was welded to the top flange. The composite beam was then put back in the fixture and tested again. In the second stage, failure was either by inelastic

Test No.	Beam	Span m (ft)	Load @	P_u kN (k)	P_e kN (k)	P_u / P_e
W-1	310x28 (W12x19)	7.3 (24)	1/2-pt.	15.6 (3.50)	10.8 (2.44)	1.43
W-2	310x33 (W12x22)	5.5 (18)	1/3-pt.	46.7 (10.5)	32.4 (7.29)	1.44
W-3	250x22 (W10x15)	5.5 (18)	1/3-pt.	18.6 (4.20)	15.1 (3.40)	1.24
W-4	310x28 (W12x19)	5.5 (18)	1/3-pt.	44.8 (10.0)	23.5 (5.28)	1.89
W-5	310x28 (W12x19)	3.7 (12)	1/2-pt.	70.3 (15.8)	56.9 (12.8)	1.23
W-6	250x22 (W10x15)	3.7 (12)	1/2-pt.	40.0 (9.00)	36.3 (8.15)	1.10
W-7	200x9.7 (M8x6.5)	3.7 (12)	1/2-pt.	8.0 (1.80)	4.8 (1.08)	1.67
W-8	200x9.7 (M8x6.5)	3.7 (12)	1/2-pt.	6.7 (1.50)	4.8 (1.08)	1.39

Notes:
 P_u is the elastic buckling load from test
 P_e is the theoretical elastic buckling load, based on $C_b = 1$

buckling or yielding and plastic hinge formation at the load point. Because of the limitations in our laboratory, it was difficult to get lengths of combined specimens long enough to produce elastic behavior. The results of all tests are shown in Tables 2 and 3 and graphically in Figures 7 and 8. Tensile coupons were taken from each member and those results are shown in Table 4.

Figure 9 shows a beam being loaded. Note the end fixtures that prevent rotation about the longitudinal axis but allows rotation about the x and y axes. Figure 10 shows a beam with channel cap after buckling. Note that the load at mid-span is applied uniformly across the flange, rather than at a ball-joint as in Figure 9. This was to see if the loading device had any restraining effect on lateral-torsional buckling.

Evaluation of Test Results

In Figures 7 and 8, the test results are plotted against the theoretical solution described in the early pages of this paper. Note that all rolled beams *without* a channel cap buckled

elastically, while most of those *with* a channel cap either buckled inelastically or formed a plastic hinge.

Note the test load/predicted load in Table 2. The predicted load was calculated using a moment diagram modifier, (called C_b in AISC) of 1.0. The P_u / P_e values then should be somewhat representative of the proper C_b values. The loading was done with a single concentrated load at either the mid-span or 1/3 point. Calculated C_b values vary from 1.32 to 1.41. With a couple of exceptions, most tests fall into this range. The average for all tests is 1.42.

The P_u / P_e values for the tests *with* channel, however, are much lower, ranging from 0.93 to 1.23 with an average of 1.10. This indicates that the current formula for C_b in the 1993 AISC-LRFD Specification is accurate enough for bisymmetric sections, but *overestimates* the value of the moment coefficient for monosymmetric sections.

Nethercot and Rockey (1971) proposed a moment modifier that was dependent on where on a cross section the load was

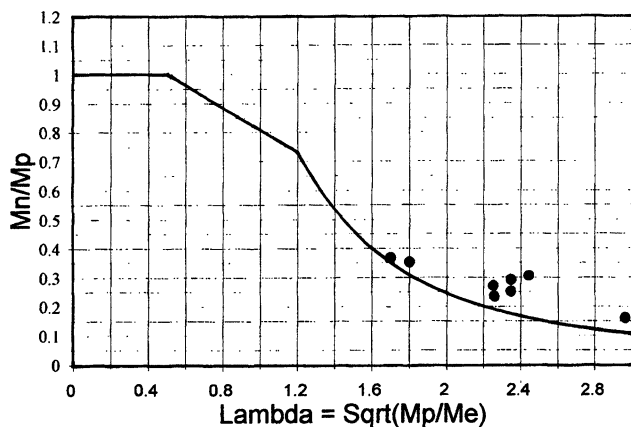


Fig. 7. Tests of rolled beams without channels.

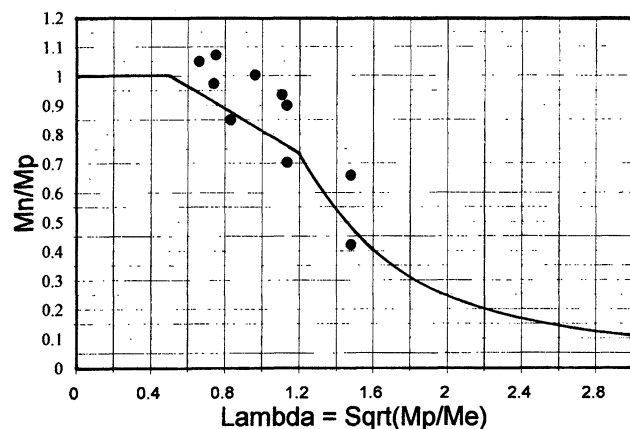


Fig. 8. Tests of beams with channel caps.

Table 3. Test Results, Beam with Channel Cap								
Test No.	Beam	Channel	Span m (ft)	Load @	P_u kN (k)	P_e kN (k)	P_u / P_e	
WC-1	310×28 (W12×19)	150×12 (C6×8.2)	7.3 (24)	1/2	53.8 (12.0)	57.8 (12.9)	0.93	
WC-1A	310×28 (W12×19)	150×12 (C6×8.2)	5.5 (18)	1/2	84.5 (19.0)	N/A		
WC-2	310×33 (W12×22)	150×12 (C6×8.2)	5.5 (18)	1/3	136 (30.5)	148 (33.3)	0.93	
WC-2A	310×33 (W12×22)	150×12 (C6×8.2)	5.5 (18)	1/3	173 (39.0)	N/A		
WC-3	250×22 (W10×15)	150×12 (C6×8.2)	5.5 (18)	1/3	102 (22.9)	81.8 (18.4)	1.23	
WC-4	310×28 (W12×19)	150×12 (C6×8.2)	5.5 (18)	1/3	158 (35.5)	128 (28.8)	1.23	
WC-5	310×28 (W12×19)	150×12 (C6×8.2)	3.7 (12)	1/2	220 (49.5)	222 (49.9)	0.99	
WC-6	250×22 (W10×15)	150×12 (C6×8.2)	3.7 (12)	1/2	145 (32.5)	125 (28.2)	1.15	
WC-7	200×9.7 (M8×6.5)	100×8 (C4×5.4)	3.7 (12)	1/2	44.5 (10.0)	36.3 (8.16)	1.23	
WC-8	200×9.7 (M8×6.5)	100×8 (C4×5.4)	3.7 (12)	1/2	40.0 (9.0)	36.3 (8.16)	1.10	

Notes:
 P_e in this table is either the plastic bending load or the inelastic buckling load, based on the LRFD straight line transition.
 The "A" subscript refers to those tests in which the load was applied through a flat surface in contact with the entire compression flange, as opposed to a ball joint.

applied. It consisted of two terms A and B , and C_b was computed as:

$$C_b = A / B \text{ if load is applied to top flange}$$

$$C_b = A \text{ if load is applied at centroid}$$

$$C_b = A \cdot B \text{ if load is applied to bottom flange}$$

They derived values for A and B for the case of a concentrated load at the mid-span of a doubly symmetric section. While this does not exactly fit the beams described in this paper, it seems to offer a plausible explanation for the values of P_u / P_e from Table 3.

A SUGGESTED DESIGN PROCEDURE

The standard unbraced length vs. moment capacity curve for doubly symmetric sections as published in AISC is shown in Figure 11. It is completely defined by M_p , M_r , L_p , L_r and the elastic buckling curve, all of which are easily calculated for rolled shapes whose properties are found in tables.

For monosymmetric sections, everything about the curve becomes more complicated. M_r is the smaller of $F_L S_{xc}$ and $F_y S_{xt}$; some vital section properties have to be calculated, with

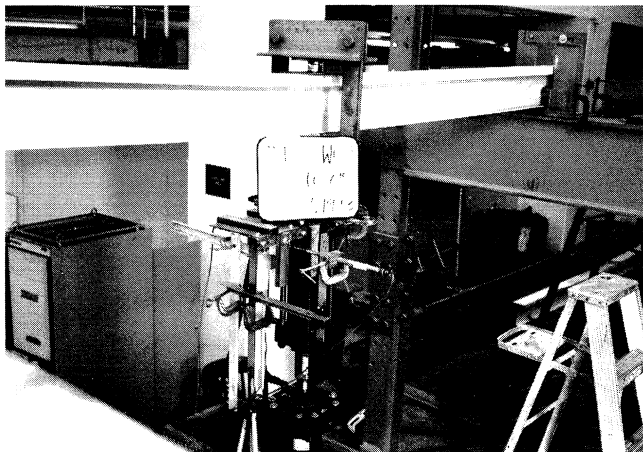


Fig. 9. Channel-capped beam under load.
 Note the end restraints against rotation
 and the top-flange, ball-joint load.

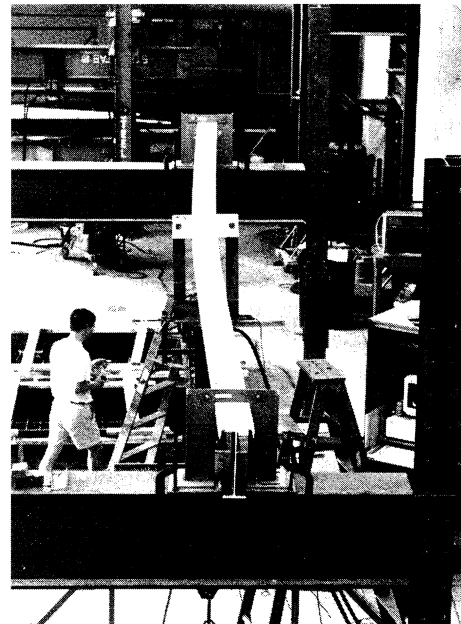


Fig. 10. Test beam after loading, showing buckled shape.

Table 4. Mechanical Properties of Test Specimens			
Beams	F_y	Channels	F_y
310×28 (W12×19)	432 MPa (62.1 ksi)	150×12 (C6×8.2)	435 MPa (62.6 ksi)
310×33 (W12×22)	431 (64.0)	150×12 (C6×8.2)	334 (48.0)
250×22 (W10×15)	370 (53.3)	150×12 (C6×8.2)	350 (50.3)
200×9.7 (M8×6.5)	278 (40.0)	100×8 (C4×5.4)	316 (45.4)

no small effort; L_r cannot be determined directly, but is the result of an iterative process.

One can help things a bit by initializing the curve, dividing M_n by M_p and changing the horizontal axis from L_b to $\lambda = \sqrt{M_p/M_e}$, where M_e is the elastic lateral-torsional buckling moment. Using the forms of β_x , C_{wc} , and J presented in this paper (Equations 11, 12, and 13), and developing curves for all 48 combination sections from AISC LRFD (pp. 1-106, 107) and AISC ASD (pp. 1-83, 85), it was found that, with small error, "one curve fits all." There is a narrow band between L_p and L_r , but the elastic curves were practically identical. This led to the approximate curve shown in Figure 12.

This eliminates the iteration to find L_r , but also obscures the unbraced length a bit. With this curve, you will have to calculate M_e for a given unbraced length, determine λ , then M_n is either M_p , M_e , or

$$M_n = M_p - (M_p - M_r) \left(\frac{\lambda - 0.49}{1.15 - 0.49} \right) \quad (22)$$

DESIGN EXAMPLE

There are two design examples attached to this report. The beam, channel cap, and span are the same as the example in the AISC Steel Design Guide Series #7—*Industrial Buildings: Roofs to Column Anchorage*, (p. 52). It is a W27×94

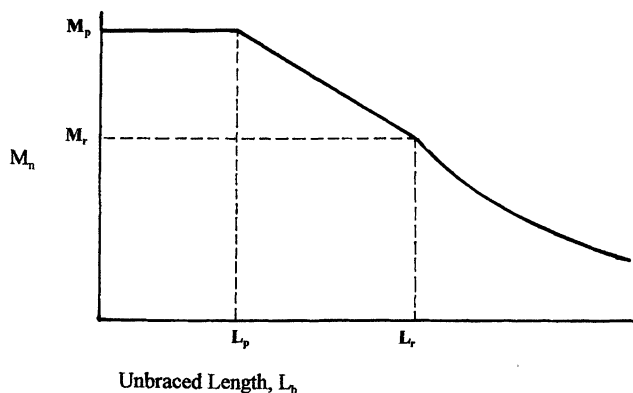


Fig. 11. Nominal moment capacity curve according to AISC-LRFD Specification.

with a C15×33.9 cap on a 30-foot simple span. It is assumed that the entire span length is unbraced laterally.

The first example makes use of the curve-fit properties of β_x , C_{wc} , and J (Equations 11, 12, and 13) of this report. This provides, of course, only an *elastic* buckling solution. For the inelastic case, it is assumed that the AISC straight-line transition between L_p and L_r is appropriate.

In calculating M_r , there is a fundamental question that must be addressed: What residual stress is appropriate? The Specification requires 10 ksi for rolled sections and 16.5 for welded shapes, but does not say what to use if you weld two rolled shapes together. The welding of a channel to the top flange of a crane beam is usually intermittent—it only being required to transmit horizontal shear, which is low. A 2- or 3-in. weld every 4 feet is usually adequate. In the author's opinion, this is not a great amount of heat input to the beam and it seems reasonable to use 10 ksi for the residual stresses in the M_r calculation.

The determination of L_r in Example 1 is still troublesome. There is no way to calculate it directly: It must be iterated, until the unbraced length used in the elastic buckling formulation produces an $M_e = M_r$. That length is then L_r .

Example 2 uses the generalized approach discussed which plots M_n/M_p against $\sqrt{M_p/M_e}$. This has the advantage of eliminating the annoying iterations for L_r , but the disadvantage of somewhat camouflaging the unbraced length.

The procedure is: calculate M_e as described herein for

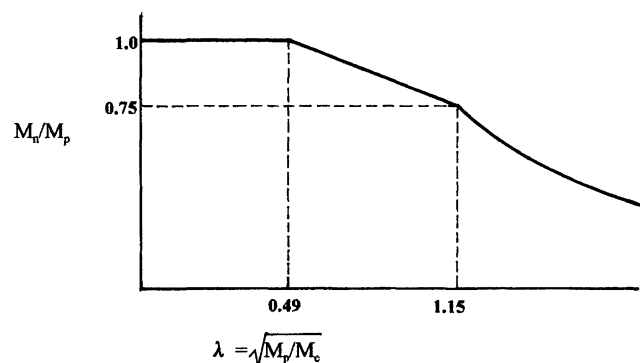


Fig. 12. Generalized M - λ curve for rolled beams with channel cap (A36 steel).

whatever unbraced length you have, then calculate λ . If λ is between 1.15 and 0.49, use the straight line transition shown in Equation 22; if it is less than 0.49, $M_n = M_p$; if it is greater than 1.15, $M_n = M_e$. Note that the results of the two examples differ by only 1 percent.

SUMMARY AND CONCLUSIONS

A mathematical model was developed to predict the elastic buckling capacity of a hot-rolled wide flange beam with a channel cap, using only those section properties that can be found in steel manuals. The cumbersome calculation of a warping constant has been reduced to a simple function of handbook properties.

Full scale tests were made on beams without channels. These specimens were chosen with unbraced lengths and cross-sections designed to ensure elastic buckling. The average of test load/calculated load was 1.42. After testing, channels were welded to the top flanges of all these beams and tested again. This time the average test/calculated load was 1.10.

The calculated buckling loads assumed $C_b = 1$, so the test/calculated values roughly correspond to the correct C_b values. Because the shear center and centroid do not coincide in the monosymmetric shapes, the C_b indicated is somewhat lower than would be calculated by the current AISC Specification. This suggests that, in the absence of more testing, it might be appropriate to take C_b as 1.0 for monosymmetric sections.

ADDITIONAL COMMENTS

Another aspect of this problem, (not a part of the research reported herein) is the restraining effect of the crane runway on the *other* side of the aisle. The maximum wheel load occurs when the trolley and lifted load is all the way to one side. Because most cranes have double-flanged wheels, the runway beam on the other side, being very lightly loaded, will add its buckling resistance in the same way a stable column supports a "leaning" column. This was not a part of the University of Florida research. In fact, this author knows of no physical tests of this phenomenon, but it makes one wonder if lateral-torsional buckling of a crane runway beam can really occur in a normally-proportioned girder, given the lateral support from the other side.

REFERENCES

- American Institute of Steel Construction, *Manual of Steel Construction, Allowable Stress Design*, 9th Ed., Chicago, IL, 1989.
- American Institute of Steel Construction, *Manual of Steel Construction, Load and Resistance Factor Design*, 2nd Ed., Chicago, IL, 1993.
- Clark J. W., and Hill, H. N., "Lateral Buckling of Beams,"

Journal of the Structural Division, ASCE, Vol. 86, No. ST7, 1960, pp. 175–196.

Galambos, T. V., *Structural Members and Frames*, Prentice-Hall, Englewood Cliffs, NJ, 1968, pp. 80–158.

Galambos, T. V., *Guide to Stability Design Criteria for Metal Structures*, Wiley, NY, 1988, pp. 155–188.

Johnston, B. G., *Guide to Stability Design Criteria for Metal Structures (SSRC)*, Wiley, NY, 1976, pp. 95–115.

Kitipornchai, S., and Trahair, N. S., "Buckling Properties of Monosymmetric I-beams," *Journal of the Structural Division*, ASCE, Vol. 106, No. ST5, 1980, pp. 941–957.

Lue, D. M., and Ellifritt, D. S., "The Warping Constant for the W-Section with a Channel Cap," *Engineering Journal*, AISC, 1st Qtr., 1993, pp. 31–33.

Nethercot, D. A., and Rockey, K. C., "A Unified Approach to the Elastic Lateral Buckling of Beams," *The Structural Engineer*, Vol. 49, No. 7, London, UK, 1971, pp. 321–330.

NOMENCLATURE

- E = Young's Modulus—200 MPa (29,000 ksi)
 G = Shear Modulus—80 MPa (11,300 ksi)
 L_b = Unbraced Length mm (in.)
 I_x, I_y = Moments of inertia about x and y, axis, respectively, mm⁴ (in.⁴)
 I_{yc} = Moment of inertia of compression flange about y-axis
 D = Depth of Rolled Beam, mm (in.)
 D_L = Depth of Lip on Channel Cap, mm (in.)
 C_w = Warping Constant of Rolled Beam, mm⁶ (in.⁶)
 C_{wc} = Warping Constant of Rolled Beam with Channel Cap
 A_c = Area of Channel, mm² (in.²)
 A_w = Area of Rolled Beam, mm² (in.²)
 J = Torsional Constant, mm⁴ (in.⁴)
 I_{yw} = Moment of inertia of rolled beam about y-axis, mm⁴ (in.⁴)
 I_{xc} = Moment of inertia of channel about its local x-axis, mm⁴ (in.⁴)
 β_x = Monosymmetry Parameter
 K = Effective Length Factors
 M_p = Plastic Moment
 M_e = Elastic Buckling Moment
 M_n = Nominal Moment Capacity
 $M_r = (F_y - F_r)S_{xc}$
- $$\lambda = \sqrt{\frac{M_p}{M_e}}$$

APPENDIX

Example 1

W27×94: $A_w = 27.7 \text{ in.}^2$, $I_{yw} = 124 \text{ in.}^4$ $C_w = 21,300 \text{ in.}^6$
 C15×33.9: $A_c = 9.96 \text{ in.}^2$, $I_{xc} = 315 \text{ in.}^4$ $b_f = D_L = 3.4 \text{ in.}$

(This is the example used by Fisher in the AISC Steel Design Guide Series #7, *Industrial Buildings*, p. 53)

$$L_b = 30 \text{ ft}$$

Warping Constant, C_{wc} (from Equation 12)

$$\begin{aligned} C_{wc} &= C_w \left(0.79 + 1.79 \sqrt{\frac{A_c}{A_w}} \right) \\ &= 21,300 \left(0.79 + 1.79 \sqrt{\frac{9.96}{27.7}} \right) \\ &= 39,690 \text{ in.}^6 \quad (1.066 \times 10^{13} \text{ mm}^6) \end{aligned}$$

Monosymmetry Parameter, β_x (from Equation 11)

$$I_{yc} = \frac{I_{yw}}{2} + I_{xc} = \frac{124}{2} + 315 = 377 \text{ in.}^4 \quad (1.57 \times 10^8 \text{ mm}^4)$$

$$\frac{I_{yc}}{I_y} = \frac{377}{439} = 0.859$$

$$R = 2 \times 0.859 = 1.718$$

$$\beta_x = 0.87(R - 1)(D + D_L/2)$$

$$= 0.87(1.718 - 1) \left(26.92 + \frac{3.4}{2} \right) = 17.88 \text{ in.} \quad (454 \text{ mm})$$

Torsion Constant, J (from Equation 15)

$$J = J_w + J_c + b_f t_1 t_2 (t_1 + t_2)$$

$$b_f = \text{flange width} = 9.99 \text{ in.} \quad (255 \text{ mm})$$

$$t_1 = \text{flange thk} = 0.745 \text{ in.} \quad (19 \text{ mm})$$

$$t_2 = \text{channel web thk} = 0.40 \text{ in.} \quad (10 \text{ mm})$$

$$K = 1.0$$

$$J = 4.03 + 1.02 + 9.99 \times 0.745 \times 0.40 (0.745 + 0.40)$$

$$= 8.46 \text{ in.}^4 \quad (3.52 \times 10^6 \text{ mm}^4)$$

$$B_1 = \frac{\pi \beta_x}{2KL} \sqrt{\frac{EI_y}{GJ}} = \frac{2.527 \beta_x}{L} \sqrt{\frac{I_y}{J}}$$

$$= \frac{2.527}{360} \times 17.88 \sqrt{\frac{439}{8.46}} = 0.9042$$

$$B_2 = \frac{\pi^2 EC_{wc}}{L^2 GJ} = \frac{25.56 C_{wc}}{L^2 J}$$

$$= \frac{25.56 \times 39,690}{(360)^2 \times 8.459} = 0.925$$

$$\begin{aligned} M_e &= \frac{\pi C_b}{KL} \left\{ \sqrt{EI_y GJ} \left(B_1 + \sqrt{1 + B_2 + B_1^2} \right) \right\} \\ &= \frac{56,600}{L} \sqrt{I_y J} \left(B_1 + \sqrt{1 + B_2 + B_1^2} \right) \\ &= \frac{56,600}{360} \sqrt{439 \times 8.46} \left(0.904 + \sqrt{1 + 0.925 + (0.904)^2} \right) \\ &= 24,530 \text{ in-k or } 2044 \text{ ft-k} \quad (2773 \text{ kN-m}) \end{aligned}$$

$$M_r = F_L S_{xc} \text{ or } F_y S_{xt}$$

$$= (36 - 10) \frac{436}{12}$$

$$= 945 \text{ ft-k} \quad (1282 \text{ kN-m}) \text{ or}$$

$$\frac{36}{12} \times 268 = 804 \text{ ft-k} \quad (1091 \text{ kN-m})$$

$$L_r = 51.6 \text{ ft} \quad (15.8 \text{ m}) \text{ (from iteration)}$$

$$M_p = \frac{36}{12} \times 357 = 1071 \text{ ft-k} \quad (1453 \text{ kN-m})$$

$$r_{yc} = \sqrt{\frac{377}{9.96 + 10 \times 0.745}} = 4.65 \text{ in.} \quad (118 \text{ mm})$$

$$L_p = \frac{300 r_{yc}}{\sqrt{F_y}} = \frac{300 \times 4.65}{12 \sqrt{36}} = 19.4 \text{ ft} \quad (5.9 \text{ m})$$

$$\begin{aligned} M_n &= M_p - (M_p - M_r) \left(\frac{L_b - L_p}{L_r - L_p} \right) \\ &= 1071 - (1071 - 804) \left(\frac{30 - 19.4}{51.6 - 19.4} \right) \\ &= \underline{983} \text{ ft-kips} \quad (1334 \text{ kN-m}) \end{aligned}$$

Example 2

Using M_e from Example 1, calculate λ

$$\lambda = \sqrt{\frac{M_p}{M_e}} = \sqrt{\frac{1071}{2044}} = .724$$

$$0.49 < \lambda < 1.15, \therefore \text{ use Equation 22}$$

$$\begin{aligned} M_n &= M_p - (M_p - M_r) \left(\frac{\lambda - 0.49}{1.15 - 0.49} \right) \\ &= 1071 - (1071 - 804) \left(\frac{0.724 - 0.49}{1.15 - 0.49} \right) \\ &= \underline{976} \text{ ft-k} \quad (1324 \text{ kN-m}) \end{aligned}$$